

Identification, Synthesis, and Characterization of New Glycogen Phosphorylase Inhibitors Binding to the Allosteric AMP Site

Marit Kristiansen,^{*,†} Birgitte Andersen,[‡] Lars Fogh Iversen,[§] and Niels Westergaard^{‡,||}

Novo Nordisk A/S, Novo Nordisk Park, DK-2760 Måløv, Denmark

Received December 3, 2003

Inhibition of glycogen phosphorylase (GP) has attracted considerable attention during the last five to 10 years as a means of treating the elevated hepatic glucose production seen in patients with type 2 diabetes. Several different GP inhibitors binding to various binding sites of the GP enzyme have been reported in the literature. In this paper we report on a novel class of compounds that have been identified as potent GP inhibitors. Their synthesis, mode of binding to the allosteric AMP site as well as *in vitro* data on GP inhibition are shown. The most potent inhibitor was found to be 4-[2,4-bis-(3-nitrobenzoylamino)phenoxy]phthalic acid (**4j**) with an IC_{50} value of 74 nM. This compound together with a closely related analogue was further characterized by enzyme kinetics and in primary rat hepatocytes.

Introduction

Type 2 diabetes is a heterogeneous disorder characterized by hyperglycaemia, which is the result of both impaired insulin secretion and insulin resistance in target tissues.¹ Numerous studies have shown that hepatic glucose production (HGP) is increased both under postabsorptive (fasted) and postprandial (fed) conditions, and, moreover, it is now increasingly recognized that elevated HGP is the major contributor to hyperglycaemia of the diabetic state.^{2–4} Using improved tracer methods, most studies find that basal HGP is elevated by 10–30% in patients with fasting blood glucose of 8–9 mM and even higher in patients with higher fasting blood glucose due to significant renal glucose loss.^{5,6} Hepatic glucose can be produced from either gluconeogenesis (the synthesis of glucose from 3-carbon precursors) or from glycogenolysis (the breakdown of glycogen). Which of these two pathways are the most predominant for the production of hepatic glucose in the diabetic state has been a matter of controversy⁷ resulting in various approaches for pharmacological intervention targeting gluconeogenesis^{8,10} and glycogenolysis.^{8,10}

Hepatic insulin resistance is suggested to lead to lack of depression on glycogenolysis⁹ and therefore glycogen phosphorylase (GP) inhibitors have attracted considerable attention during the last five to 10 years because of their potential use for the treatment of type 2 diabetes.^{7,10} This has been shown both *in vitro* using cultured hepatocytes^{11,12} and in type 2 diabetic animal models^{13,14} and humans.¹⁵ Glycogen phosphorylase catalyses the phosphohydrolysis of glycogen to yield glucose-1-phosphate and this is the rate-limiting step in the overall process of glycogen degradation. In the liver, glucagon stimulates glycogen degradation via a

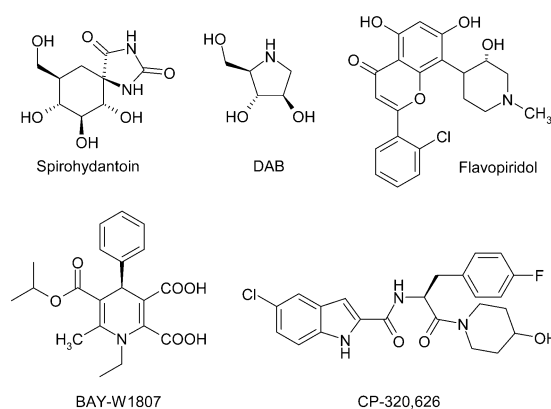


Figure 1. Examples of GP inhibitors that bind at the different sites of the GP enzyme.

cascade of events, resulting in covalent modification of GP by phosphorylation (at Ser14) into its active form, which is termed GP_a.¹⁶ Dephosphorylation of GP_a to its inactive form, termed GP_b, is mediated by protein phosphatases.^{17,18} Both GP_a and GP_b can exist in an inactive conformation, the T-state, and an active conformation, the R-state.^{19–21} Allosteric effectors, especially AMP, are also important for the activity of muscle GP_b, which can be activated to 80% of the GP_a activity by stabilizing the more active R-state.^{22,23}

There are several known binding sites in the GP-enzyme: the catalytic site, the inhibitor (or nucleoside) site, the AMP allosteric (or nucleotide) site, the glycogen storage site, and a new allosteric site.^{7,10,24,25} The first class of nonphysiological inhibitors of GP described were the glucose analogues.^{26–29} These inhibitors bind to the catalytic site and one of the most potent compounds is a spirohydantoin (Figure 1), which inhibits rabbit muscle GP_b with a K_i value of 3 μ M.²⁶ Other inhibitors binding at the catalytic site are the iminosugars. Earlier we reported a group of piperidines within this series as potent inhibitors of GP,³⁰ however, the most potent compound, 1,4-dideoxy-1,4-imino-D-arabinitol, DAB (Figure 1), inhibits liver GP_a with a K_i value of 400 nM.¹³ Caffeine and other heteroaromatic compounds bind to

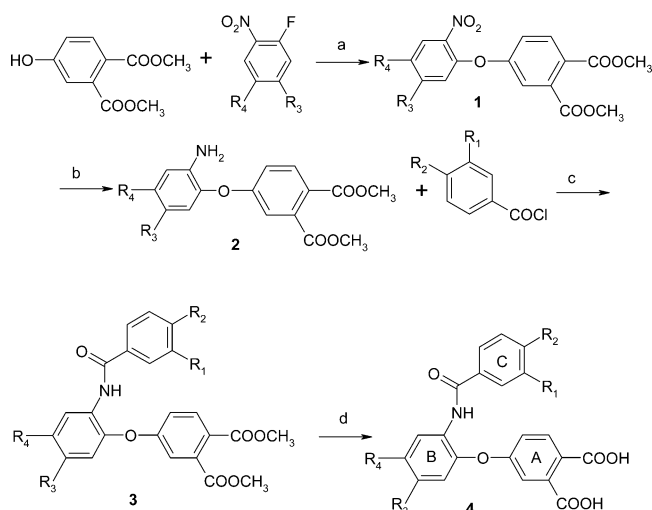
* To whom the correspondence should be addressed. Phone: +45 4443 4855. Fax: +45 4466 3939. E-mail: mkri@novonordisk.com.

[†] Medicinal Chemistry Research II.

[‡] Hepatic Biochemistry.

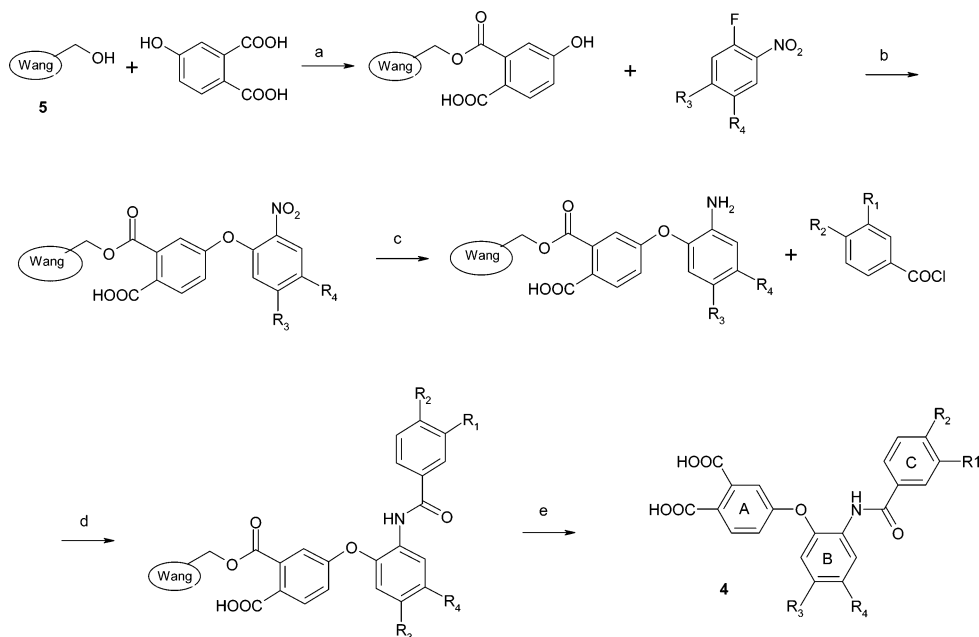
[§] Protein Science.

^{||} Present address: LEO Pharma A/S, Industriparken 55, DK-2750 Ballerup, Denmark.

Scheme 1^a

^a Reagents and conditions: (a) K_2CO_3 , DMF, 100 °C. (b) H_2 , Pd/C, CH_2Cl_2 , room temp. (c) TEA, acetone. (d) 2 N NaOH, dioxane, room temp.

the inhibitor site. Flavopiridol (Figure 1) is one of the most potent compounds within this class and inhibits rabbit muscle GPb with an IC_{50} value of 1 μM .³¹ Glycogen phosphorylase inhibitors that bind to the allosteric site have also been reported. BAY-W1807 (Figure 1) was until recently the most potent in this class with a K_i value, in the absence of AMP, of 11 nM³² (muscle GPa); however, a phthalic acid derivative with an IC_{50} (human liver GPa) of 1 nM has just been published.³³ A few years ago a new allosteric site was discovered. Different indole derivatives, e.g., CP-320,626 (Figure 1), were found to bind to this new site, and IC_{50} values were reported to be in the low nM range (human liver GPa).^{14,34–36} It still remains unclear which of the preciously described binding sites that will be the most beneficial for pharmacological intervention.¹² Also, one has to be cautious, when comparing data from various

Scheme 2^a

^a Reagents and conditions: (a) DIC, DMAP, DMF, room temp. (b) 0.5 M potassium bis(trimethylsilyl)amide, DMF. (c) Tin(II) chloride, NMP. (d) DIC, DMF, CH_2Cl_2 . (e) CH_2Cl_2 , TFA (1:1).

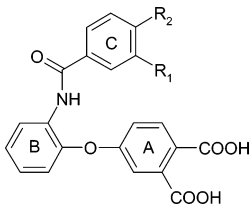
laboratories, since several species, tissue isoforms, phosphorylation states, and GP activity assay (glycogenolysis or glycogen synthesis) have been used to evaluate inhibitors. Especially the role of glucose and AMP for the potency of these inhibitors needs to be explored. For example, glucose is known to potentiate the inhibitory action of caffeine,³⁷ whereas AMP is known to increase the K_i value for glucose.³⁸ This suggests that the simultaneous presence of both AMP and glucose could be determining for the potency of various inhibitors.^{12,14,27,28,39}

In this paper we report structure–activity relationship (SAR) and kinetic data of a series of compounds that have been identified as GP inhibitors and which bind to the AMP-binding site as shown by protein crystallography. In addition, the effect of glucose and AMP on the potency of compound **4a** was investigated.

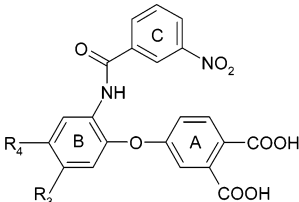
Chemistry

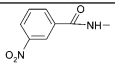
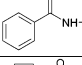
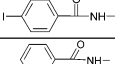
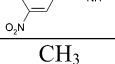
Compound **4a** was identified as a GPa inhibitor by high-throughput screening and was synthesized as outlined in Scheme 1 ($R_1 = NO_2$, $R_2 = R_3 = R_4 = H$). The phenoxyphthalate **1a** was prepared by reaction of dimethyl 4-hydroxyphthalate with 2-fluoronitrobenzene. The resulting nitrophenoxy-phthalate was reduced with hydrogen in the presence of Pd/C in methylene chloride to give the aminophenoxy-phthalate **2a**, which was reacted with 3-nitrobenzoyl chloride to give **3a**. Hydrolysis of **3a** with 2 N sodium hydroxide in dioxane gave compound **4a** ($R_1 = NO_2$, $R_2 = R_3 = R_4 = H$).

A library of analogues of **4a** having different substituents in the B- or the C-phenyl ring was prepared using a solid-phase method starting from the commercially available Wang resin **5** as described in Scheme 2. Successive 1,3-diisopropylcarbodiimide (DIC)-mediated coupling with 4-hydroxyphthalic acid, reaction with different analogues of *o*-fluoronitrobenzene, reduction of the nitro group with tin(II) chloride, DIC-mediated coupling with different benzoic acids, and finally tri-

Table 1. IC₅₀ Values of **4a–i** Using Pig Liver GP and Rabbit Muscle GP


compd	R ₁	R ₂	GP _a liver (μM)	GP _b muscle (μM)
4a	NO ₂	H	1.3	0.9
4b	Cl	H	41	6
4c	OCH ₃	H	~40	50
4d	COCH ₃	H	~70	50
4e	H	H	>200	~100
4f	COOH	H	>100	>200
4g	Cl	Cl	>50	
4h	H	Cl	>200	
4i	H	CH ₃	>30	
CP-320,626 ^a			2.4	0.5

^a CP-320,626 from Pfizer was used as control.**Table 2.** IC₅₀ Values for **4j–u** in Pig Liver GP_a


Compd	R ₃	R ₄	GP _a liver (nM)
4j	H		74
4k	H		120
4l	H		90
4m	CH ₃		700
4n	H	CH ₃	450
4o	H	F	2500
4p	H	Br	250
4q	H	CF ₃	1800
4r	H	CH ₃ (CO)NH	140
4s	H	CH ₃ O(CO)	1200
4t	H	CN	2200
4u	CH ₃	H	90

fluoroacetic acid (TFA) resin cleavage gave the desired products. Compounds **4b–u** (Tables 1 and 2) were prepared by either of the two methods (Scheme 1 and Scheme 2).

Results and Discussion

As compound **4a** was identified by high-throughput screening, no binding site data existed for this type of compound. To identify the binding site and interactions with the enzyme, GP_b was cocrystallized with compound **4a**. A single electron density peak was identified in a difference Fourier map which showed that compound **4a** occupied the allosteric AMP binding pocket of GP (see Figure 2A and 2B). Compound **4a** was found not to bind elsewhere. Although the allosteric AMP site is

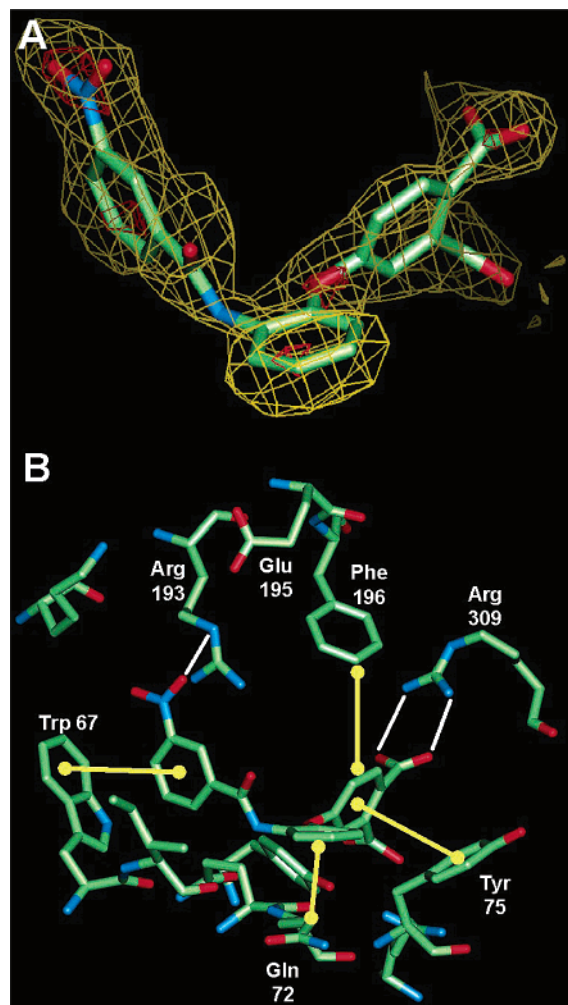


Figure 2. **4a** in the allosteric AMP binding pocket of GP_b. (A) The $2F_o - F_c$ electron density map for **4a** found in the allosteric AMP site contoured at one sigma level in yellow and at three sigma in red. (B) The interaction of compound **4a** with the various residues in the AMP site. Hydrogen bonds are indicated (in white) and van der Waals interactions are in yellow.

known as an activation site, the GP inhibitor **4a**, however, clearly binds in a different mode compared to AMP (see Figure 3A and 3B). **4a** thus induces conformational changes upon binding to the GP_b enzyme; hence, the enzyme was found in the inactive T-conformation (not shown), in a similar way as reported for the GP inhibitor BAY-W1807 from Bayer.⁴⁰

Table 1 shows the ability of compound **4a–i** to inhibit the activity of pig liver GP_a and rabbit muscle GP_b measured in the direction of glycogenolysis. Data for the known GP inhibitor, CP-320,626¹² (Figure 1), is included for comparison. Modifications in the C-ring resulted in loss of potency, especially when using the pig liver GP_a isozyme. This correlated well with the structural data, as the C-ring is buried in the AMP site. The B-ring, however, was found to be located at the outer part of the AMP binding pocket with the R₃ and R₄ position available for substitution and with direction out of the AMP binding pocket and pointing toward the other GP molecule in the GP homodimer. Thus, when a substituent in the B-ring was introduced (Table 2), the potency increased by severalfold with compound **4j** being the most potent one having an IC₅₀ value of 74 nM.

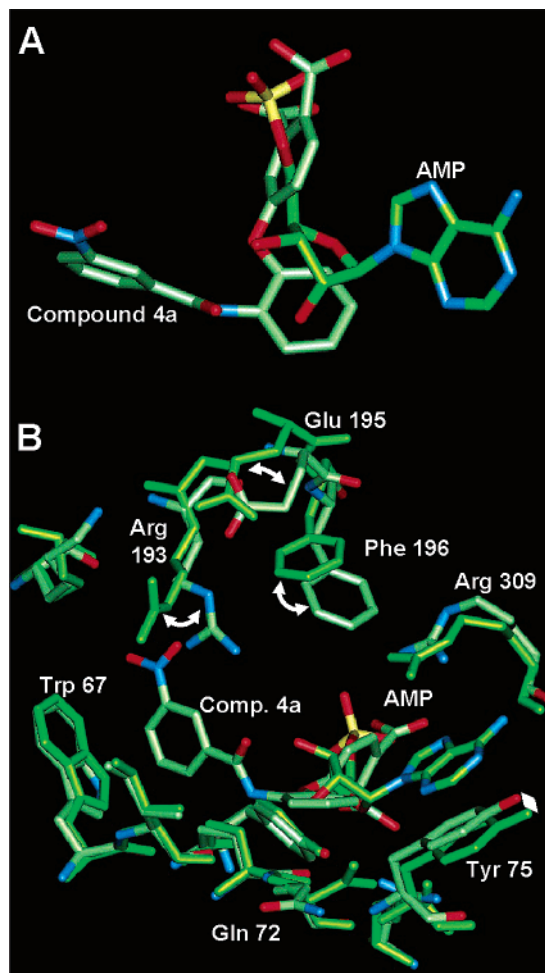


Figure 3. AMP in the allosteric AMP binding pocket of GPb. The structures of **4a** and AMP (PDB code 8GPB) were superimposed and the AMP site depicted (**4a** in standard colors and AMP in light green). (A) **4a** and AMP alone. (B) The full AMP site; the major movements in the pocket are indicated with white arrows.

Compound **4j** was also cocrystallized with GPb and as expected the R₄ substituent was extending outward from the AMP binding pocket, making contact with the other GP molecule in the GP homodimer (Figure 4). Hence, compound **4j** makes contacts to both GP molecules in the homodimer and this could explain the increase in potency of **4j** compared to, for example, **4a**.

Figure 5 shows the dose–response curves for inhibition of pig liver GP_a and rabbit muscle GP_b when measured in the direction of glycogenolysis using compounds **4j** and **4a**. As can be seen, both compounds are potent inhibitors with **4j** being 18 and 41 times more potent than **4a** in inhibiting liver GP_a and muscle GP_b, respectively. To study the effect of glucose on the potency of these types of compounds dose–response curves were generated for **4a** in the presence of 0–6 mM glucose and measured in the direction of glycogen synthesis. It has been reported previously that BAY–W1807³² acts in synergism with glucose similar to what has been shown for caffeine.³⁷ Likewise it can be seen (Figure 6A) that glucose synergistically increased the potency of **4a** using pig liver GP_a. The maximal synergistic effect was obtained at 5–6 mM glucose where the IC₅₀ value was 50% of the initial value. This is thus consistent with the findings for BAY–W1807. Since **4a**

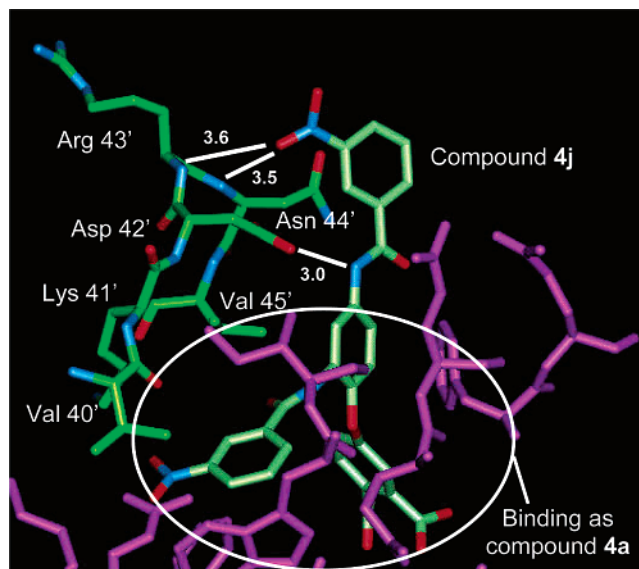


Figure 4. Compound **4j** (shown in standard colors) in the GPb homodimer. In magenta the GPb monomer where compound **4j** binds such as compound **4a** (identical interactions as shown in Figure 2B). Residues 40–43 of the second monomer in the GPb homodimer are depicted (carbon atoms in light green and nitrogen/oxygen in standard colors). The novel contacts (as compared to compound **4a**) are shown.

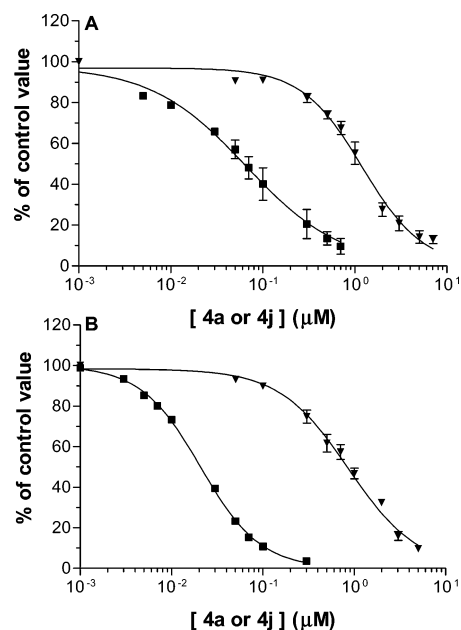


Figure 5. Pig liver GP_a (A) and rabbit muscle GP_b (B) were measured in the direction of glycogen degradation using 2 mg/mL glycogen as the substrate in the presence of increasing concentrations of **4j** (■) or **4a** (▼). The IC₅₀ values (μM) for **4j** and **4a** were calculated to be 0.074 ± 0.015 μM (3) and 1.3 ± 0.2 μM (5) on pig liver GP_a and 0.87 ± 0.13 μM (3) and 0.21 μM (1) on rabbit muscle GP_b, respectively. Results are averages ± SEM of the number of experiments given in parentheses.

was found to bind to the AMP binding site, dose–response curves were generated in order to investigate the effect of AMP on the potency of **4a** both in the presence and in absence of 6 mM glucose. Figure 6B shows that AMP increased the IC₅₀ values of **4a** in a dose-dependent fashion, i.e., the potency decreased. However, in the presence of 6 mM glucose this effect was less profound. In this context it should be noted

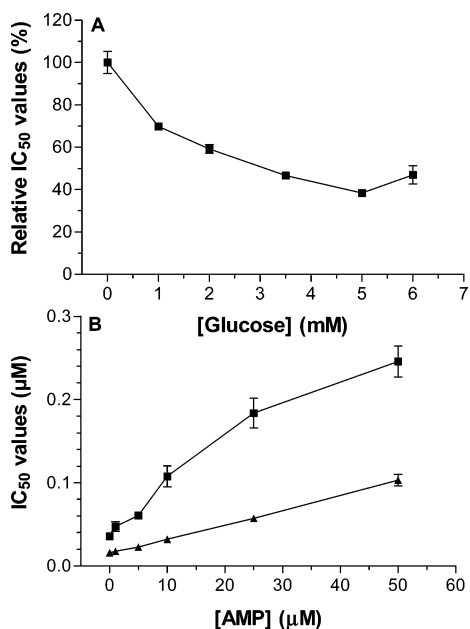


Figure 6. Pig liver GPa was assayed in the direction of glycogen synthesis. (A) The effect of increasing concentrations of glucose on the potency of **4a** on pig liver GPa was measured. 100% corresponds to an IC₅₀ value of 34 ± 2 nM. (B) The potency of **4a** was measured with increasing concentrations of AMP in the presence (▲) or absence (■) of 6 mM glucose. Results are average of three individual experiments \pm SEM.

that the IC₅₀ value is severalfold lower compared to when the inhibition is measured in the direction of glycogenolysis. This is also found for other types of GP inhibitors¹² binding to various binding sites, and therefore caution must be exercised when the potency of GP inhibitors is compared.

To characterize the effect of the two compounds, **4a** and **4j**, in a cell model system, the inhibitors were tested in cultured primary rat hepatocytes. The effect of the two compounds on glycogenolysis with respect to glucose and glycogen is shown in Figure 7. Glucagon (0.5 nM) increased the glucose production 2.1-fold (Figure 7A). **4j** was also found to be the most potent compound in the hepatocytes. From Figure 7A, the IC₅₀ values for **4j** for inhibition of basal and glucagon-induced glycogenolysis were calculated to be 1.6 ± 0.2 µM and 4.7 ± 0.3 µM, respectively. The IC₅₀ values for **4a** for inhibition of basal and glucagon-induced glucose production were calculated (Figure 7A) to be 9.8 ± 2.4 µM and 30.0 ± 4.5 µM, respectively. The IC₅₀ values for inhibition of glucagon-induced glycogenolysis is increased approximately 3-fold compared to inhibition of basal glycogenolysis. This is in agreement with the increased AMP level found when cells are stimulated with glucagon. The increase in cAMP caused by glucagon will spontaneously break down to AMP by phosphodiesterases. The intracellular concentration of AMP in a basal state has been reported to approximately 500 µM in rat liver.³⁹ At this concentration of AMP, GP is fully saturated^{39,41} and inhibitors binding to the AMP site are expected to be less potent compared to the situation where AMP is absent (Figure 6). This may explain why the potency of **4a** and **4j** was less profound using cultured hepatocytes. This also has to be considered when GP inhibitors are designed for pharmacological intervention. The glycogen levels in the hepatocytes

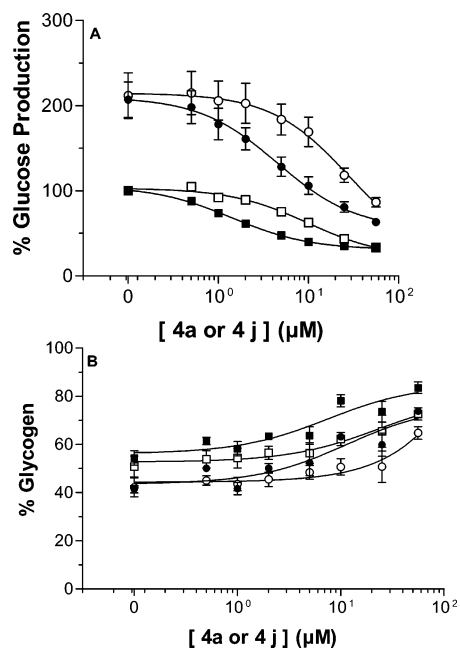


Figure 7. Effect of **4a** and **4j** on basal and glucagon-induced glycogenolysis. (A) Basal (■, □) and glucagon-induced (0.5 nM) (●, ○) glucose production were measured over 70 min. Open symbols **4a**, closed symbols **4j**. Basal glucose production was set to 100% and equals 269 ± 12 nmol glucose/mg protein \times 70 min. (B) Glycogen levels after basal (■, □) and glucagon-induced (●, ○) glycogenolysis were determined. Open symbols **4a**, closed symbols **4j**. Glycogen level before start of the experiment was set to 100% and equals 2604 ± 367 nmol glycosyl unit/mg protein. All results are means \pm SEM of four separate hepatocyte isolation.

after incubation with the two compounds are shown in Figure 7B. The glycogen content of the hepatocytes was measured to 2600 nM \pm 370 nmol glycosyl unit/mg protein before initiation of glycogenolysis, and this is set to 100% in Figure 7B. The IC₅₀ values calculated from Figure 7B are not significantly different from the IC₅₀ values calculated from Figure 7A.

In summary, we have discovered a class of GP inhibitors that bind to the allosteric AMP binding site. On the basis of SAR and crystallography data, the potency of this class of compounds was increased by creating an interaction with both GP monomers in the GP homodimer, leading to compound **4j**. Furthermore, compound **4j** inhibits glycogenolysis in primary rat hepatocytes.

The best binding site for pharmacological intervention of GP inhibitors is difficult to predict. However, as shown in this paper, the intracellular concentrations of glucose and AMP have to be taken into consideration for GP inhibitors binding to the AMP binding site. Thus future studies will show if **4j** can lower blood glucose in an animal model of type 2 diabetes as well.

Experimental Section

Materials. Reagents and solvents were obtained from commercial suppliers and used without further purification. Solvents used were either AR or HPLC grade. Dry DMF was prepared and stored over molecular sieves (3 Å).

General Chemistry. Melting points (uncorrected) were measured on a Büchi B545 apparatus. ¹H and ¹³C NMR spectra were recorded on a Bruker Advance DPX 200 MHz instrument unless otherwise noted. Chemical shifts are given in ppm (δ) relative to TMS and coupling constants are in Hz. The HPLC-

MS analyses were performed on a PE Sciex API 100 LC/MS system using a Waters 3 mm \times 150 mm, 3.5 μ m, C-18 Symmetry column and a positive ion spray with a flow rate of 20 μ L/min. The column was eluted with a linear gradient 10% to 100% A, in 7.5 min at a flow rate of 1.5 mL/min (Solvent A = acetonitrile, 0.01% TFA). Detection: 210 nm. The elemental composition of the compounds agrees to within $\pm 0.4\%$ of the calculated value. The HPLC purifications were performed on a Gilson instrument with two Gilson 306 pumps equipped with 25 mL SC pump heads, Gilson 806 manometer, and Gilson 811c dynamic mixing chamber. UV detection was performed with Gilson 119 UV/VIS detector. Gilson 215 Nebula was used as combined injector and fraction collector. Analytical HPLC was performed on a Merck-Hitachi with a Waters Xterra MS, 3 mm \times 50 mm, 3.5 μ m, C-18 column. The column was eluted with a linear gradient 0% to 100% B, in 7 min at a flow rate of 1.2 mL/min (Solvent A = 5% acetonitrile and 0.01% TFA diluted with water to 100%; solvent B = acetonitrile). Detection: 210 nm.

4-(2-Nitrophenoxy)phthalic Acid Dimethyl Ester (1a). A mixture of 4-hydroxyphthalic acid dimethyl ester (1.25 g, 5.95 mmol), *o*-fluoronitrobenzene (0.81 mL, 7.64 mmol), and potassium carbonate (1.66 g, 12 mmol) in dry DMF (25 mL) was heated at 100 $^{\circ}$ C for 1 h. The mixture was cooled to room temperature and filtered and the filtrate evaporated to dryness in vacuo to give the crude product of **1a** as a yellow oil (Yield: 1.97 g (100%)). The compound was used in the next step without further purification. $^1\text{H NMR}$ (CDCl_3) in ppm: δ 3.9 (6H, 2 \times s), 7.1–7.2 (2H, m), 7.2 (1H, $J = 2.9$ Hz, d), 7.3–7.4 (1H, m), 7.6–7.7 (1H, m), 7.84 (1H, $J = 8.2$ Hz, d), 8.03 (1H, $J = 1.8$ and 8.2 Hz, dd). $^{13}\text{C NMR}$ (CDCl_3) in ppm: δ 168.1 (CO), 167.0 (CO), 159.5, 148.6, 142.4, 135.8, 135.2, 132.0, 126.4, 126.4, 125.8, 123.1, 119.8, 117.8, 53.2, 53.0.

4-(2-Aminophenoxy)phthalic Acid Dimethyl Ester (2a). 4-(2-Nitrophenoxy)phthalic acid dimethyl ester, **1a** (10 g, 30.2 mmol), was dissolved in methylene chloride (500 mL). 10% Pd/C (450 mg) was added, and the mixture was hydrogenated for 19 h at 30 psi. The reaction mixture was filtered and evaporated to dryness in vacuo. **2a** was obtained as an oil (Yield: 8.5 g (93%)). $^1\text{H NMR}$ (CDCl_3) in ppm: δ 3.86 (3H, s), 3.90 (3H, s), 6.7–6.97 (3H, m), 7.0–7.1 (2H, m), 7.15 (1H, $J = 2.0$ Hz, d), 7.78 (1H, $J = 8.3$ Hz, d). $^{13}\text{C NMR}$ (CDCl_3) in ppm: δ 52.9; 53.2; 116.5; 117.4; 118.2; 119.4; 121.6; 124.4; 126.7; 132.1; 136.1; 139.2; 141.6; 160.8; 167.1; 168.8.

4-[2-(3-Nitrobenzoylamino)phenoxy]phthalic Acid Dimethyl Ester (3a). A solution of 3-nitrobenzoyl chloride (0.43 g, 2.3 mmol) in dry acetone (2 mL) was added slowly to a solution of 4-(2-aminophenoxy)phthalic acid dimethyl ester, **2a** (0.63 g, 2.09 mmol) and TEA (0.35 mL, 2.5 mmol) in dry acetone (2 mL) at 0 $^{\circ}$ C. The mixture was stirred at room temperature for 20 h and filtered and the filtrate evaporated to dryness in vacuo. The crude product was purified on silica gel (Eluent: methylene chloride: ethyl acetate (95:5)) to give **3a** as a golden oil (Yield: 1.19 g (47%)). $^1\text{H NMR}$ (CDCl_3) in ppm: δ 3.9 (6H, 2 \times s), 7.02 (1H, $J = 1.6$ and 8.5 Hz, dd), 7.1–7.25 (2H, m), 7.25–7.35 (2H, m), 7.7 (1H, $J = 8.0$ Hz, t), 7.83 (1H, $J = 8.5$ Hz, d), 8.1 (1H, $J = 1.1$ and 8.0 Hz, dt), 8.3 (1H, br s), 8.4 (1H, m), 8.54 (1H, $J = 1.6$ and 8.0 Hz, dd), 8.65 (1H, m). $^{13}\text{C NMR}$ (CDCl_3) in ppm: δ 53.1, 53.3, 118.0, 119.6, 119.8, 122.6, 123.2, 125.9, 126.0, 126.3, 126.9, 129.9, 130.5, 132.2, 133.2, 136.1, 136.6, 145.2, 148.7, 159.4, 163.5, 166.9, 168.1. If needed, the compound could be further purified by precipitation as a mixed hydrochloride and acetate salt. Anal. ($\text{C}_{16}\text{H}_{15}\text{NO}_5 \cdot \text{HCl} \cdot \frac{1}{2}\text{HOAc}$) C, H, N.

Preparation of Compounds 3b, 3e, 3f. The compounds were prepared in a similar way as described for compound **3a**. The crude products were isolated and used as such in the next step.

4-[2-(3-Chlorobenzoylamino)phenoxy]phthalic Acid Dimethyl Ester (3b). Yield: 100% crude product. LC/MS: m/z : 408 ($\text{M} - \text{CH}_3\text{O}$), 440 (MH^+). $^1\text{H NMR}$ (CDCl_3) in ppm: δ 3.9 (6H, 2 \times s), 6.98 (1H, $J = 1.8$ and 8.0 Hz, dd), 7.1–7.2 (2H, m), 7.23–7.35 (2H, m), 7.4 (1H, $J = 8.0$ Hz, d), 7.48–

7.65 (2H, m), 7.8 (1H, $J = 2.0$ Hz, t), 7.83 (1H, $J = 8.5$ Hz, d), 8.27 (1H, br s), 8.55 (1H, $J = 1.8$ and 8.5 Hz, dd).

4-(2-Benzoylamino)phthalic Acid Dimethyl Ester (3e). Yield: 100% crude product. LC/MS: m/z : 375 ($\text{M} - \text{CH}_3\text{O}$), 406 (MH^+). $^1\text{H NMR}$ (CDCl_3) in ppm: δ 3.9 (6H, 2 \times s), 6.98 (1H, $J = 1.8$ and 8.7 Hz, dd), 7.08–7.2 (2H, m), 7.23–7.35 (2H, m), 7.4–7.6 (3H, m), 7.75–7.78 (2H, m), 7.83 (1H, $J = 8.7$ Hz, d), 8.3 (1H, br s), 8.63 (1H, $J = 1.8$ and 8.4 Hz, dd).

4-[2-(3-Ethoxycarbonylbenzoylamino)phenoxy]phthalic Acid Dimethyl Ester (3f). Yield: 100% crude product. $^1\text{H NMR}$ (CDCl_3) in ppm: δ 1.4 (3H, $J = 6.9$ Hz, t), 3.9 (6H, 2 \times s), 4.40 (2H, $J = 6.9$ Hz, q), 6.98 (1H, $J = 1.8$ and 8.7 Hz, dd), 7.10–7.33 (4H, m), 7.56 (1H, $J = 8.0$ Hz, t), 7.83 (1H, $J = 8.7$ Hz, d), 7.97 (1H, $J = 1.6$ and 8.0 Hz, dt), 8.20 (1H, $J = 1.4$ and 8.3 Hz, dt), 8.30 (1H, br s), 8.45 (1H, $J = 1.6$ Hz, t), 8.60 (1H, $J = 1.8$ and 8.3 Hz, dd).

4-[2-(3-Nitrobenzoylamino)phenoxy]phthalic Acid (4a). Sodium hydroxide (2 N, 12 mL) was added to a solution of 4-[2-(3-nitrobenzoylamino)phenoxy]phthalic acid dimethyl ester, **3a** (1.15 g, 2.83 mmol) in 1,4-dioxane (12 mL) at room temperature. The mixture was stirred for 2 h and cooled to < 10 $^{\circ}$ C and the pH adjusted to 2–3 with 1 N HCl (approximately 24 mL). The resulting crystals were filtered off and washed with water. The crystals were dried to give beige crystals of **4a** (Yield: 0.82 g (76%)). LC-MS m/z 423 (MH^+). $^1\text{H NMR}$ ($\text{DMSO}-d_6$) in ppm: δ 10.3 (1H, s), 8.58 (1H, m), 8.38 (1H, m), 8.18 (1H, $J = 7.8$ Hz, d), 7.6–7.8 (3H, m), 7.3–7.4 (2H, m), 7.18 (1H, $J = 1.9$ and 7.6 Hz, dd), 7.1 (1H, m), 7.07 (1H, $J = 2.5$ and 8.5 Hz, dd). $^{13}\text{C NMR}$ ($\text{DMSO}-d_6$) in ppm: δ 116.6, 118.4, 120.8, 122.3, 125.0, 126.1, 127.3, 127.5, 129.4, 130.0, 133.0, 133.8, 135.5, 136.0, 147.6, 148.6, 158.8, 164.5, 167.3, 168.1. mp: 200–202 $^{\circ}$ C. Anal. ($\text{C}_{21}\text{H}_{14}\text{N}_2\text{O}_8$) C, H, N.

Preparation of Compounds 4b, 4e, 4f. The compounds were prepared in a similar way as described for compound **4a**.

4-[2-(3-Chlorobenzoylamino)phenoxy]phthalic Acid (4b). Yield: 69%. mp: 194–195 $^{\circ}$ C. LC-MS: m/z 412 (MH^+), 394 ($\text{MH}^+ - \text{H}_2\text{O}$). $^1\text{H NMR}$ ($\text{DMSO}-d_6$) in ppm: δ 10.0 (1H, s), 8.1 (1H, br s), 7.7 (4H, m), 7.58 (1H, $J = 8.0$ Hz, d), 7.45 (1H, m), 7.27 (2H, m), 7.1 (1H, $J = 7.5$ Hz, d), 7.02 (1H, $J = 2.5$ and 8.5 Hz, dd). Anal. ($\text{C}_{21}\text{H}_{14}\text{ClNO}_6$) C, H, N.

4-(2-Benzoylamino)phthalic Acid (4e). Yield: 42% (97.4% purity by HPLC). LC-MS: m/z 378 (MH^+), 360 ($\text{MH}^+ - \text{H}_2\text{O}$). $^1\text{H NMR}$ ($\text{DMSO}-d_6$) in ppm: δ 9.8 (1H, s), 8.16 (1H, $J = 8.5$ Hz, d), 7.77 (1H, m), 7.71–7.74 (3H, m), 7.52 (1H, $J = 7.0$ Hz, t), 7.43 (2H, $J = 7.5$ Hz, t), 7.26 (2H, m), 7.11 (1H, m), 7.05 (1H, $J = 2.5$ and 8.5 Hz, dd).

4-[2-(3-Carboxyphenylcarbamoyl)phenoxy]phthalic Acid (4f). Yield: 47%. (97.1% purity by HPLC). mp: 235–237 $^{\circ}$ C. LC/MS: m/z 467 ($\text{M} + 2\text{Na}$), 404 ($\text{MH}^+ - \text{H}_2\text{O}$). $^1\text{H NMR}$ ($\text{DMSO}-d_6$) in ppm: δ 10.2 (1H, s), 8.4 (1H, $J = 1.5$ Hz, t), 8.1 (1H, $J = 7.6$ Hz, d), 8.02 (1H, $J = 7.6$ Hz, d), 7.65–7.8 (2H, m), 7.6 (1H, $J = 8.1$ Hz, t), 7.3 (2H, m), 7.2 (1H, m), 7.13 (1H, $J = 2.5$ and 8.6 Hz, dd).

Preparation of 4-[2-(3-Methoxybenzoylamino)phenoxy]phthalic Acid (4c). To a suspension of Wang resin (1 g, 0.92 mmol, Bachem, loading: 0.92 mmol/g) in a mixture of methylene chloride (5 mL) and DMF (5 mL) were added 4-hydroxyphthalic acid (1.7 g, 9.3 mmol), 1,3-diisopropylcarbodiimide (1.4 mL, 9.0 mmol), and 4-(dimethylamino)pyridine (66 mg, 0.54 mmol). The mixture was shaken for 20 h and filtered. The resin was washed with DMF (4 \times 10 mL), methylene chloride (4 \times 10 mL), methanol (4 \times 10 mL), and methylene chloride (4 \times 10 mL). The resin was dried in vacuo. *o*-Fluoronitrobenzene (0.4 mL, 3.77 mmol) and 0.5 M potassium bis(trimethylsilyl)amide (1.2 mL, 0.6 mmol) were added to a suspension of the dried resin in DMF (4 mL). The mixture was shaken for 24 h under a nitrogen atmosphere and filtered. The resin was washed with DMF (4 \times 5 mL), methylene chloride (4 \times 5 mL), DMF (4 \times 5 mL), and *N*-methylpyrrolidone (NMP) (4 \times 5 mL). A solution of tin(II) chloride dihydrate (0.9 g, 3.99 mmol) in NMP (4 mL) was added to the resin. The mixture was shaken for 24 h, filtered, and washed with NMP (4 \times 5 mL), methylene chloride (4 \times 5 mL), and methanol (4 \times 5 mL). The resin was dried in vacuo to give approximately 244 mg of material.

To a suspension of this resin (50 mg, 0.046 mmol) in a mixture of DMF (0.5 mL) and methylene chloride (0.5 mL) were added 3-methoxybenzoic acid (80 mg, 0.526 mmol) and 1,3-diisopropylcarbodiimide (40 μ L, 0.257 mmol). The mixture was shaken for 24 h and filtered and the resin washed with DMF (4 \times 4 mL), THF (4 \times 4 mL), and methylene chloride (4 \times 4 mL). The resin was shaken with methylene chloride:TFA (1:1) (1 mL) for 20 min. The mixture was filtered and the resin washed with carbon tetrachloride (4 mL), and the collected filtrates were evaporated to dryness in vacuo to give **4c** (20 mg, yield: 96%) as a brownish oil. The oil was further purified on HPLC: The oil was dissolved in 2200 μ L of acetonitrile to which one drop of DMSO was added. HPLC purification was performed on Nucleosil C-18 7 μ m 8 \times 100 mm columns (packed by Grom). A standard gradient with water/acetonitrile with 0.01% TFA was used. Flow rate 9 mL/min starting at 10% organic modifier ending after 18 min on 100% modifier. This condition was kept for 1 min. Fractions of 4 mL were collected in a deep-well collection plate. Evaporation of the solvent in vacuo gave **4c** (98% purity by HPLC). LC-MS: *m/z* 408 (MH⁺), 390 (MH⁺ - H₂O). ¹H NMR (DMSO-*d*₆) in ppm: δ 9.95 (1H, s), 7.73 (2H, m), 7.27–7.40 (5H, m), 7.19 (1H, m), 7.11 (2H, m), 7.09 (1H, *J* = 2.5 and 8.6 Hz, dd), 3.8 (3H, s).

Preparation of Compounds 4d and 4g–u. The compounds were prepared in a similar way as described for compound **4c**.

4-[2-(3-Acetylbenzoylamino)phenoxy]phthalic Acid (4d). LC-MS: *m/z* 420 (MH⁺), 402 (MH⁺ - H₂O). ¹H NMR (CD₃OD) in ppm: δ 8.24 (1H, br s), 8.11 (1H, *J* = 7.6 Hz, d), 7.89 (1H, *J* = 8.1 Hz, d), 7.80 (1H, *J* = 2.0 and 7.6 Hz, dd), 7.72 (1H, *J* = 8.6 Hz, d), 7.62 (1H, *J* = 8.1 Hz, t), 7.35 (2H, m), 7.16–7.22 (2H, m), 7.09 (1H, *J* = 2.5 and 8.6 Hz, dd), 2.57 (3H, s). 96% purity by HPLC.

4-[2-(3,4-Dichlorobenzoylamino)phenoxy]phthalic Acid (4g). LC-MS: *m/z* 428/430 (MH⁺ - H₂O). ¹H NMR (DMSO-*d*₆) in ppm: δ 10.02 (1H, s), 7.96 (1H, br s), 7.73–7.76 (3H, m), 7.71 (1H, *J* = 1.5 and 7.1 Hz, dd), 7.34 (2H, m), 7.19 (1H, *J* = 2.0 and 7.6 Hz, dd), 7.11 (1H, m), 7.09 (1H, *J* = 2.5 and 8.6 Hz, dd). 98% purity by HPLC.

4-[2-(4-Chlorobenzoylamino)phenoxy]phthalic Acid (4h). LC-MS: *m/z* 412 (MH⁺), 394 (MH⁺ - H₂O). ¹H NMR (DMSO-*d*₆) in ppm: δ 9.9 (1H, s), 8.07 (1H, m), 7.80 (2H, *J* = 8.5 Hz, d), 7.65–7.8 (2H, m), 7.50 (2H, *J* = 8.5 Hz, d), 7.26 (2H, m), 7.10 (1H, *J* = 7.5 Hz, d), 7.02 (1H, *J* = 2.5 and 9.0 Hz, dd). 96% purity by HPLC.

4-[2-(4-Methylbenzoylamino)phenoxy]phthalic Acid (4i). LC-MS: *m/z* 392 (MH⁺), 374 (MH⁺ - H₂O). ¹H NMR (DMSO-*d*₆) δ 9.8 (1H, s), 7.76 (2H, m), 7.69 (2H, *J* = 8.1 Hz, d), 7.31 (2H, m), 7.27 (2H, *J* = 8.1 Hz, d), 7.16 (2H, m), 7.08 (1H, *J* = 2.5 and 8.6 Hz, dd). 96% purity by HPLC.

4-[2,4-Bis-(3-nitrobenzoylamino)phenoxy]phthalic Acid (4j). LC-MS: *m/z* 587 (MH⁺), 569 (MH⁺ - H₂O). ¹H NMR (DMSO-*d*₆) δ 10.8 (1H, s), 10.45 (1H, s), 8.83 (1H, br s), 8.58 (1H, br s), 8.4 (3H, m), 8.24 (1H, *J* = 1.8 Hz, d), 8.19 (1H, *J* = 8.1 Hz, d), 7.86 (1H, *J* = 8.1 Hz, t), 7.76 (3H, m), 7.25 (1H, *J* = 8.1 Hz, d), 7.09 (1H, *J* = 2.5 and 8.6 Hz, dd), 7.08 (1H, s). mp: 184–186 °C. Anal. (C₂₈H₁₈N₄O₁₁) C, H, N.

4-[4-Benzoylamino-2-(3-nitrobenzoylamino)phenoxy]phthalic Acid (4k). LC-MS: *m/z* 524 (MH⁺ - H₂O) ¹H NMR (DMSO-*d*₆) in ppm: δ 10.42 (1H, s), 10.38 (1H, s), 8.5 (1H, s), 8.37 (1H, *J* = 8.1 Hz, d), 8.18 (1H, *J* = 2.5 Hz, d), 8.15 (1H, *J* = 7.6 Hz, d), 7.96 (2H, *J* = 7.1 Hz, d), 7.73 (2H, m), 7.67 (1H, *J* = 8.3 Hz, d), 7.5–7.62 (3H, m), 7.2 (1H, *J* = 8.8 Hz, d), 7.02–7.1 (2H, m). 100% purity by HPLC.

4-[4-(4-Iodobenzoylamino)-2-(3-nitrobenzoylamino)phenoxy]phthalic Acid (4l). LC-MS: *m/z* 668 (MH⁺), 650 (MH⁺ - H₂O). ¹H NMR (DMSO-*d*₆) in ppm: δ 10.47 (1H, s), 10.39 (1H, s), 8.56 (1H, s), 8.39 (1H, *J* = 8.0 Hz, d), 8.15–8.21 (2H, m), 7.94 (2H, *J* = 8.3 Hz, d), 7.68–7.8 (5H, m), 7.22 (1H, *J* = 8.8 Hz, d), 7.09 (2H, m). 100% purity by HPLC.

4-[5-Methyl-2,4-bis-(3-nitrobenzoylamino)phenoxy]phthalic Acid (4m). LC-MS: *m/z* 601 (M+1), 583 (MH⁺ - H₂O). ¹H NMR (DMSO-*d*₆) in ppm: δ 10.35 (1H, s), 8.75 (1H, s), 8.46 (1H, s), 8.42 (1H, *J* = 8.1 Hz, d), 8.37 (1H, *J* = 7.6 Hz,

d), 8.33 (1H, *J* = 8.6 Hz, d), 8.1 (1H, *J* = 8.1 Hz, d), 7.82 (1H, *J* = 8.1 Hz, t), 7.66–7.2 (3H, m), 7.08–7.13 (3H, m). 100% purity by HPLC.

4-[4-Methyl-2-(3-nitrobenzoylamino)phenoxy]phthalic Acid (4n). LC-MS: *m/z* 437 (MH⁺), 419 (MH⁺ - H₂O). ¹H NMR (DMSO-*d*₆) in ppm: δ 10.28 (1H, s), 8.55 (1H, s), 8.38 (1H, *J* = 8.3 Hz, d), 8.16 (1H, *J* = 7.8 Hz, d), 7.75 (1H, *J* = 7.8 Hz, t), 7.7 (1H, *J* = 8.8 Hz, d), 7.5 (1H, s), 7.17 (1H, *J* = 8.0 Hz, d), 7.0–7.1 (3H, m), 2.8 (3H, s). 100% purity by HPLC.

4-[4-Fluoro-2-(3-nitrobenzoylamino)phenoxy]phthalic Acid (4o). LC-MS: *m/z* 441 (MH⁺), 423 (MH⁺ - H₂O). ¹H NMR (DMSO-*d*₆) in ppm: δ 10.44 (1H, s), 8.54 (1H, s), 8.39 (1H, *J* = 2.2 and 8.6 Hz, dd), 8.15 (1H, *J* = 8.9 Hz, d), 7.76 (1H, *J* = 8.9 Hz, t), 7.65–7.73 (2H, m), 7.27 (1H, m), 7.19 (1H, m), 7.05–7.1 (2H, m). >98% purity by HPLC.

4-[4-Bromo-2-(3-nitrobenzoylamino)phenoxy]phthalic Acid (4p). LC-MS: *m/z* 483/485 (MH⁺ - H₂O). ¹H NMR (DMSO-*d*₆) in ppm: δ 10.46 (1H, s), 8.56 (1H, s), 8.4 (1H, *J* = 2.2 and 8.1 Hz, dd), 8.17 (1H, *J* = 7.8 Hz, d), 7.96 (1H, *J* = 2.5 Hz, d), 7.76 (1H, *J* = 8.1 Hz, t), 7.72 (1H, *J* = 8.3 Hz, d), 7.51 (1H, *J* = 2.5 and 8.8 Hz, dd), 7.1–7.18 (3H, m). 100% purity by HPLC.

4-[2-(3-Nitrobenzoylamino)-4-trifluoromethylphenoxy]phthalic Acid (4q). LC-MS: *m/z* 491 (MH⁺), 473 (MH⁺ - H₂O). ¹H NMR (DMSO-*d*₆) in ppm: δ 10.58 (1H, s), 8.64 (1H, s), 8.43 (1H, *J* = 2.2 and 8.3 Hz, dd), 8.25 (1H, *J* = 8.2 Hz, d), 8.17 (1H, s), 7.74–7.84 (2H, m), 7.68 (1H, *J* = 2.0 and 8.8 Hz, dd), 7.31 (1H, *J* = 8.8 Hz, d), 7.19–7.27 (2H, m). >98% purity by HPLC.

4-[4-Acetylamino-2-(3-nitrobenzoylamino)phenoxy]phthalic Acid (4r). LC-MS: *m/z* 480 (MH⁺), 462 (MH⁺ - H₂O). ¹H NMR (DMSO-*d*₆) in ppm: δ 10.31 (1H, s), 10.12 (1H, s), 8.4 (1H, s), 8.31 (1H, *J* = 9.0 Hz, d), 8.05 (1H, *J* = 7.8 Hz, d), 7.89 (1H, s), 7.67 (1H, *J* = 8.1 Hz, t), 7.62 (1H, *J* = 8.5 Hz, d), 7.44 (1H, *J* = 8.8 Hz, d), 7.1 (1H, *J* = 8.8 Hz, d), 6.99 (1H, *J* = 2.5 and 8.8 Hz, dd), 6.95 (1H, s). > 98% purity by HPLC.

4-[4-Methoxycarbonyl-2-(3-nitrobenzoylamino)phenoxy]phthalic Acid (4s). LC-MS: *m/e* 481 (MH⁺), 463 (MH⁺ - H₂O). ¹H NMR (DMSO-*d*₆) in ppm: δ 10.50 (1H, s), 8.63 (1H, s), 8.42 (1H, *J* = 7.8 Hz, d), 8.35 (1H, s), 8.24 (1H, *J* = 7.6 Hz, d), 7.90 (1H, *J* = 2.2 and 8.6 Hz, dd), 7.72–7.82 (2H, m), 7.18–7.26 (3H, m). 100% purity by HPLC.

4-[4-Cyano-2-(3-nitrobenzoylamino)phenoxy]phthalic Acid (4t). LC-MS: *m/z* 430 (MH⁺ - H₂O). ¹H NMR (DMSO-*d*₆) in ppm: δ 10.58 (1H, s), 8.6 (1H, s), 8.41 (1H, *J* = 8.1 Hz, d), 8.18–8.24 (2H, m), 7.78 (2H, *J* = 8.3 Hz, d), 7.75 (1H, *J* = 2.5 and 8.6 Hz, dd), 7.28 (1H, *J* = 8.6 Hz, d), 7.2–7.25 (2H, m). 100% purity by HPLC.

4-[5-Methyl-2-(3-nitrobenzoylamino)phenoxy]phthalic Acid (4u). LC-MS: *m/z* 419 (MH⁺ - H₂O). ¹H NMR (DMSO-*d*₆) in ppm: δ 10.26 (1H, s), 8.55 (1H, s), 8.38 (1H, *J* = 8.3 Hz, d), 8.17 (1H, *J* = 7.8 Hz, d), 7.78 (1H, *J* = 7.8 Hz, t), 7.7 (1H, *J* = 8.3 Hz, d), 7.58 (1H, *J* = 8.1 Hz, d), 7.17 (1H, *J* = 8.1 Hz, d), 7.05–7.1 (2H, m), 7.0 (1H, s), 2.8 (3H, s). >98% purity by HPLC.

Biology. Enzyme Assay. Preparation of pig liver GP (GPb < 10%) was performed according to literature.¹³ Rabbit muscle GPb was obtained from Sigma Chemicals and was activated by 25 μ M AMP unless otherwise stated.

Glycogen phosphorylase activity was measured in the direction of glycogen breakdown from the photometrical determination of the rate of NADPH formation in an assay coupled to phosphoglucosylase and glucose 6-phosphate dehydrogenase (G-6-P-DH).¹³ The enzyme activity was assayed at pH 6.8 and 37 °C in a phosphate buffer containing KH₂PO₄ (18 mM), Na₂HPO₄ (27 mM), MgCl₂ (15 mM), EDTA (100 μ M), NADP⁺ (340 μ M), glucose 1,6-bisphosphate (4 μ M), G-6-P DH (6000 U/L), and phosphoglucosylase (800 U/L) using a glycogen concentration of 2 mg/mL.

In some cases the GP activity was assayed in the direction of glycogen synthesis by measuring the formation of inorganic phosphate from glucose 1-phosphate in a buffer containing *N,N*-bis[2-hydroxyethyl]-2-aminoethanesulfonic acid (BES) (50 mM), EDTA (1 mM), and glycogen (0.125%) at pH 6.8 and at

25 °C. The reaction was started with glucose 1-phosphate at concentration of 0.5 mM. The rate of inorganic phosphate formation was determined using a kit [EnzCheck, Molecular probes] (see also ref 42).

Isolation and Culturing of Hepatocytes. Primary rat hepatocytes were isolated from Male Wistar rats (~250 g) and cultured in 24-well plates as described previously.^{11,43} The hepatocytes were incubated in high glucose (15 mM) and high insulin (10 nM) to induced glycogen synthesis. After intensive wash in glucose-free buffer (117.6 mM NaCl, 5.4 mM KCl, 0.82 mM Mg₂SO₄, 1.5 mM KH₂PO₄, 20 mM HEPES, 9 mM NaHCO₃, 0.1% w/v HSA, and 2.25 mM CaCl₂, pH 7.4), the inhibitory effect of **4a** and **4j** on basal and glucagon induced (0.5 nM glucagon) glycogenolysis were studied. Glucose released into the medium was measured using a glucose oxidase kit. Glycogen levels were determined after two rapid washes of cells with ice-cold 0.9% w/v NaCl by amyloglucosidase (exo-1,4- α -D-glucosidase) digest as described by Gomez-Lechon et al.⁴⁴

Cocrystallization of GPb and Compounds 4a and 4j. Protein Purification. GPb was isolated from rabbit skeletal muscle and prepared for crystallization as previously described.⁴⁵

Crystallization. An approximately 25 mg/mL GPb solution consisting of 10 mM BES, 0.1 mM EDTA, 3 mM DTT, 1 mM spermine, pH 6.7, was prepared for crystallization. Crystals were grown by the hanging drop method using seeding as nucleation. One mmol of compound **4a** or **4j** was added to the protein solution before crystallization. Three microliters of protein–ligand solution was used per drop. The reservoir volume was 1 mL consisting of 10 mM BES, 0.1 mM EDTA, 3 mM DTT, 1 mM spermine, pH 6.7. Crystals grew to the size of 1.0 × 0.2 × 0.2 mm over 2–4 days.

Data Collection. A GPb crystal (with either compound **4a** or **4j**) of the size 1.0 × 0.2 × 0.2 mm was flash frozen at 100 K prior to data collection. The following cryo conditions were used: the crystal was removed from the hanging drop and transferred to 35% glycerol (containing 1.0 mmol inhibitor, 10 mM BES, and 0.1 mM EDTA). After a 45 s soak, the crystal was flash frozen.

Data were collected on in-house equipment (RU300, Cu K α 50 kV/100 mA). The crystal to detector distance was 200 mm. A 0.75° oscillation was used for 100 images; in total, 75° were collected. Data were collected using a 5 min exposure per image. See Supporting Information for data collection details. The space group was determined to be P₄₃,2. Data processing was performed using Denzo, Scalepack and the CCP4 program suite.^{46,47}

Refinements. The 1a8i RCSB entry (1.7 Å data, and isomorph with current data sets) was used as a starting model for phasing with water and ligand molecules omitted from the structure. All refinements were performed with X-PLOR (version 3.851) (Accelrys Inc.). Interchanging cycles of model building (QUANTA) and refinement (X-PLOR) were performed; for details, see Supporting Information. The F_o – F_c and 2F_o – F_c maps were inspected by the use of X-LIGAND (QUANTA application) for densities that could correspond to the structure of compound **4a** or **4j**. A well-suited density was identified in the allosteric AMP binding pocket. No other densities were identified to fit the inhibitors. The protein structure was inspected and corrected by the use of X-BUILD (Accelrys Inc.). Water molecules were inserted using the X-SOLVE program (Accelrys Inc.).

Supporting Information Available: Crystallographic data collection details for compound **4a** and **4j** and analytical data for all compounds, **4a–u**. This material is available free of charge via the Internet at <http://pubs.acs.org>.

References

- Cefalu, W. T. Insulin resistance: Cellular and clinical concepts. *Exp. Biol. Med.* **2001**, *226*, 13–26.
- DeFronzo, R. A.; Bonadonna, R. C.; and Ferrannini, E. Pathogenesis of NIDDM: A Balanced overview. *Diabetes Care* **1992**, *15*, 318–368.
- Lefebvre, P. J.; Scheen, A. J. Glucose metabolism and the postprandial state. *Eur. J. Clin. Invest.* **1999**, *29 Suppl 2*, 1–6.
- Tappy, L. Regulation of hepatic glucose production in healthy subjects and patients with noninsulin-dependent diabetes mellitus. *Diabetes Metab.* **1995**, *21*, 233–240.
- Rigalleau, V.; Beylot, M.; Laville, M.; Guillot, C.; Deleris, G.; Aubertin, J.; Gin, H. Measurement of post-absorptive glucose kinetics in non-insulin-dependent diabetic patients: methodological aspects. *Eur. J. Clin. Invest.* **1996**, *26*, 231–236.
- Wajngot, A.; Chandramouli, V.; Schumann, W. C.; Ekberg, K.; Jones, P. K.; Efendic, S.; Landau, B. R. Quantitative contributions of gluconeogenesis to glucose production during fasting in type 2 diabetes mellitus. *Metab., Clin. Exp.* **2001**, *50*, 47–52.
- Treadway, J. L.; Mendys, P.; Hoover, D. J. Glycogen phosphorylase inhibitors for treatment of type 2 diabetes mellitus. *Expert. Opin. Invest. Drugs* **2001**, *10*, 439–454.
- Kurukulasuriya, R.; Link, J. T.; Madar, D. J.; Pei, Z.; Richards, S. J.; Rohde, J. J.; Souers, A. J.; Szczepankiewicz, B. G. Potential drug targets and progress towards pharmacologic inhibition of hepatic glucose production. *Curr. Med. Chem.* **2003**, *10*, 123–153.
- Lewis, G. F.; Carpentier, A.; Vranic, M.; Giacca, A. Resistance to insulin's acute direct hepatic effect in suppressing steady-state glucose production in individuals with type 2 diabetes. *Diabetes* **1999**, *48*, 570–576.
- McCormack, J. G.; Westergaard, N.; Kristiansen, M.; Brand, C. L.; Lau, J. Pharmacological approaches to inhibit endogenous glucose production as a means of anti-diabetic therapy. *Curr. Pharm. Des.* **2001**, *7*, 1451–1474.
- Andersen, B.; Rassov, A.; Westergaard, N.; Lundgren, K. Inhibition of glycogenolysis in primary rat hepatocytes by 1,4-dideoxy-1,4-imino-D-arabinitol. *Biochem. J.* **1999**, *342*, 545–550.
- Andersen, B.; Westergaard, N. The effect of glucose on the potency of two distinct glycogen phosphorylase inhibitors. *Biochem. J.* **2002**, *367*, 443–450.
- Fosgerau, K.; Westergaard, N.; Quistorff, B.; Grunnet, N.; Kristiansen, M.; Lundgren, K. Kinetic and functional characterization of 1,4-dideoxy-1,4-imino-D-arabinitol: A potent inhibitor of glycogen phosphorylase with anti-hyperglycaemic effect in ob/ob mice. *Arch. Biochem.* **2000**, *380*, 274–284.
- Martin, W. H.; Hoover, D. J.; Armento, S. J.; Stock, I. A.; McPherson, R. K.; Danley, D. E.; Stevenson, R. W.; Barrett, E. J.; Treadway, J. L. Discovery of a human liver glycogen phosphorylase inhibitor that lowers blood glucose in vivo. *Proc. Natl. Acad. Sci. U.S.A.* **1998**, *95*, 1776–1781.
- Treadway, J. L.; Levy, C. B.; Hoover, D. J.; Stevenson, R. W.; Gibbs, E. M.; Gelfand, R. A.; Kuye, O. Glucose lowering by glycogen phosphorylase inhibition in rats, dogs, and humans. *Diabetes* **2001**, *50*, Suppl.2, A133.
- Sutherland, E. W.; Robison G. A. The role of cyclic AMP in the control of carbohydrate metabolism. *Diabetes* **1969**, *18*, 797–819.
- Aleman, S.; Pelech, S.; Brierley, C. H.; Cohen, P. The protein phosphatases involved in cellular regulation. Evidence that dephosphorylation of glycogen phosphorylase and glycogen synthase in the glycogen and microsomal fractions of rat liver are catalysed by the same enzyme: protein phosphatase-1. *Eur. J. Biochem.* **1986**, *156*, 101–110.
- Bollen, M.; Vandenhede, J. R.; Goris, J.; Stalmans, W. Characterization of glycogen-synthase phosphatase and phosphorylase phosphatase in subcellular liver fractions. *Biochim. Biophys. Acta* **1988**, *969*, 66–77.
- Monod, J.; Wyman, J.; Changeux, J.-P. On the nature of allosteric transitions: A plausible model. *J. Mol. Biol.* **1965**, *12*, 88–118.
- Newgard, C. B.; Hwang, P. K.; Fletterick, R. J. The family of glycogen phosphorylases: Structure and function. *Crit. Rev. Biochem. Mol. Biol.* **1989**, *24*, 69–99.
- Barford, D.; Johnson, L. N. The allosteric transition of glycogen phosphorylase. *Nature* **1989**, *340*, 609–616.
- Johnson, L. N.; Hu, S. H.; Barford, D. Catalytic mechanism of glycogen phosphorylase. *Faraday Discuss.* **1992**, *93*, 131–142.
- Buchbinder, J. L.; Rath, V. L.; Fletterick, R. J. Structural relationships among regulated and unregulated phosphorylases. *Annu. Rev. Biophys. Biomol. Struct.* **2001**, *30*, 191–209.
- Oikonomakos, N. G. Glycogen phosphorylase as a molecular target for type 2 diabetes therapy. *Curr. Protein Pept. Sci.* **2002**, *3*, 561–586.
- Somsák, L.; Nagy, V.; Hadady, Z.; Docsa, T.; Gergely, P. Glucose analogue inhibitors of glycogen phosphorylases as potential antidiabetic agents: Recent developments. *Curr. Pharm. Des.* **2003**, *9*, 1177–1189.
- Richard, C. J. F.; Mitchell, E. P.; Wormald, M. R.; Watson, K. A.; Johnson, L. N.; Zographos, S. E.; Koutra, D. D.; Oikonomakos, N. G.; Fleet, G. W. J. Potent inhibition of glycogen phosphorylase by a spirohydantoin of glucopyranose: First pyranose analogues of hydantocidin. *Tetrahedron Lett.* **1995**, *54*, 2145–2148.

- (27) Martin, J. L.; Veluraja, K.; Ross, K.; Johnson, L. N.; Fleet, G. W.; Ramsden, N. G.; Bruce, I.; Orchard, M. G.; Oikonomakos, N. G.; Papageorgiou, A. C.; Leonidas, D. D.; Tsitoura, H. S. Glucose analogue inhibitors of glycogen phosphorylase: the design of potential drugs for diabetes. *Biochemistry* **1991**, *30*, 10101–10116.
- (28) Board, M.; Hadwen, M.; Johnson, L. N. Effects of novel analogues of D-glucose on glycogen phosphorylase activities in crude extracts of liver and skeletal muscle. *Eur. J. Biochem.* **1995**, *228*, 753–761.
- (29) Oikonomakos, N. G.; Kosmopoulou, M.; Zographos, S. E.; Leonidas, D. D.; Chrysina, E. D.; Somsák, L.; Nagy, V.; Praly, J.-P.; Docsa, T.; Tóth, B.; Gergely, P. Binding of N-acetyl-N'-β-D-glucopyranosyl urea and N-benzoyl-N'-β-D-glucopyranosyl urea to glycogen phosphorylase b. *Eur. J. Biochem.* **2002**, *269*, 1684–1696.
- (30) Jakobsen, P.; Lundbeck, J. M.; Kristiansen, M.; Breinholt, J.; Demuth, H.; Pawlas, J.; Candela, M. P. T.; Andersen, B.; Westergaard, N.; Lundgren, K.; Asano, N. Iminosugars: Potential Inhibitors of Liver Glycogen Phosphorylase. *Bioorg. Med. Chem.* **2001**, *9*, 733–744.
- (31) Oikonomakos, N. G.; Schnier, J. B.; Zographos, S. E.; Skamnaki, V. T.; Tsitsanou, K. E.; Johnson, L. N. Flavopiridol inhibits glycogen phosphorylase by binding at the inhibitor site. *J. Biol. Chem.* **2000**, *275*, 34566–34573.
- (32) Oikonomakos, N. G.; Tsitsanou, K. E.; Zographos, S. E.; Skamnaki, V. T.; Goldmann, S.; Bischoff, H. Allosteric inhibition of glycogen phosphorylase a by the potential antidiabetic drug 3-isopropyl 4-(2-chlorophenyl)-1,4-dihydro-1-ethyl-2-methylpyridine-3,5,6-tricarboxylate. *Protein Sci.* **1999**, *8*, 1930–1945.
- (33) Lu, Z.; Bohn, J.; Bergeron, R.; Deng, Q.; Ellsworth, K. P.; Geissler, W. M.; Harris, G.; McCann, P. E.; McKeever, B.; Myers, R. W.; Saperstein, R.; Willoughby, C. A.; Yao, J.; Chapman, K. A new class of glycogen phosphorylase inhibitors. *Bioorg. Med. Chem. Lett.* **2003**, *13*, 4125–4128.
- (34) Hoover, D. J.; Lefkowitz-Snow, S.; Burgess-Henry, J. L.; Martin, W. H.; Armento, S.; Stock, I. A.; McPherson, R. K.; Genereux, P. E.; Gibbs, E. M.; Treadway, J. L. Indole-2-carboxamide inhibitors of human liver glycogen phosphorylase. *J. Med. Chem.* **1998**, *41*, 2934–2938.
- (35) Oikonomakos, N. G.; Chrysina, E. D.; Kosmopoulou, M. N.; Leonidas, D. D. Crystal structure of rabbit muscle glycogen phosphorylase a in complex with a potential hypoglycaemic drug at 2.0 Å resolution. *Biochim. Biophys. Acta – Proteins Proteom.* **2003**, *1647*, 325–332.
- (36) Rath, V. L.; Ammirati, M.; Danley, D. E.; Ekstrom, J. L.; Gibbs, E. M.; Hynes, T. R.; Mathiowetz, A. M.; McPherson, R. K.; Olson, T. V.; Treadway, J. L.; Hoover, D. J. Human liver glycogen phosphorylase inhibitors bind at a new allosteric site. *J. Chem. Biol.* **2000**, *7*, 677–682.
- (37) Kasvinsky, P. J.; Shechosky, S.; Fletterick, R. J. Synergistic regulation of phosphorylase a by glucose and caffeine. *J. Biol. Chem.* **1978**, *253*, 9102–9106.
- (38) Oikonomakos, N. G.; Kontou, M.; Zographos, S. E.; Watson, K. A.; Johnson, L. N.; Bichard, C. J.; Fleet, G. W.; Acharya, K. R. N-acetyl-(beta)-D-glucopyranosylamine: a potent T-state inhibitor of glycogen phosphorylase. A comparison with {alpha}-D-glucose. *Protein Sci* **1995**, *4*, 2469–2477.
- (39) Ercan-Fang, N.; Gannon, M. C.; Rath, V. L.; Treadway, J. L.; Taylor, M. R.; Nuttall, F. Q. Integrated effects of multiple modulators on human liver glycogen phosphorylase a. *Am. J. Physiol. Endocrinol. Metab.* **2002**, *283*, E29–E37.
- (40) Zographos, S. E.; Oikonomakos, N. G.; Tsitsanou, K. E.; Leonidas, D. D.; Chrysina, E. D.; Skamnaki, V. T.; Bischoff, H.; Goldmann, S.; Watson, K. A.; Johnson, J. L. The structure of glycogen phosphorylase b with an alkyl-dihydropyridine-dicarboxylic acid compound, a novel and potent inhibitor. *Structure* **1997**, *5*, 1413–1425.
- (41) Westergaard, N. Unpublished results.
- (42) Sergienko, E. A.; Srivastava D. K. A continuous spectrophotometric method for the determination of glycogen phosphorylase-catalyzed reaction in the direction of glycogen synthesis. *Anal. Biochem.* **1994**, *221*, 348–355.
- (43) Seglen, P. O. Preparation of isolated rat liver cells. *Methods Cell. Biol.* **1976**, *13*, 29–83.
- (44) Gomez-Lechon, P. X.; Castell, J. V. A microassay for measuring glycogen in 96-well-cultured cells. *Anal. Biochem.* **1996**, *236*, 296–301.
- (45) Tsitsanou, K. E.; Oikonomakos, N. G.; Zographos, S. E.; Skamnaki, V. T.; Gregoriou, M.; Watson, K. A.; Johnson, L. N.; Fleet, G. W. J. Effects of commonly used cryoprotectants on glycogen phosphorylase activity and structure. *Protein Sci.* **1999**, *8*, 741–749.
- (46) Otwinowski, Z.; Minor, W. Processing of X-ray diffraction data collected in oscillation mode. *Methods Enzymol.* **1997**, *276*, 307–326.
- (47) Collaborative Computational Project, Number 4. The CCP4 suite: Programs for protein crystallography. *Acta Crystallogr. Sect. D.* **1994**, *D50*, 760–763.

JM031121N